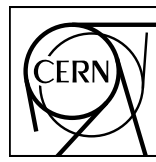


EUROPEAN ORGANIZATION FOR NUCLEAR RESEARCH



CERN-EP-2022-055

17 March 2022

System-size dependence of the charged-particle pseudorapidity density at $\sqrt{s_{\text{NN}}} = 5.02 \text{ TeV}$ for pp, p–Pb, and Pb–Pb collisions

ALICE Collaboration*

Abstract

We present the first systematic comparison of the charged-particle pseudorapidity densities for three widely different collision systems, pp, p–Pb, and Pb–Pb, at the top energy of the Large Hadron Collider ($\sqrt{s_{\text{NN}}} = 5.02 \text{ TeV}$) measured over a wide pseudorapidity range ($-3.5 < \eta < 5$), the widest possible among the four experiments at that facility. The systematic uncertainties are minimised since the measurements are recorded by the same experimental apparatus (ALICE). The distributions for p–Pb and Pb–Pb collisions are determined as a function of the centrality of the collisions, while results from pp collisions are reported for inelastic events with at least one charged particle at midrapidity. The charged-particle pseudorapidity densities are, under simple and robust assumptions, transformed to charged-particle rapidity densities. This allows for the calculation and the presentation of the evolution of the width of the rapidity distributions and of a lower bound on the Bjorken energy density, as a function of the number of participants in all three collision systems. We find a decreasing width of the particle production, and roughly a smooth ten fold increase in the energy density, as the system size grows, which is consistent with a gradually higher dense phase of matter.

© 2022 CERN for the benefit of the ALICE Collaboration.

Reproduction of this article or parts of it is allowed as specified in the CC-BY-4.0 license.

*See Appendix A for the list of collaboration members

1 Introduction

The number of charged particles produced in energetic nuclear collisions is an important indicator for the strong interaction processes that determine the particle production at the sub-nucleonic level. In particular, the production of charged particles is expected to reflect the number of quark and gluon collisions occurring during the initial stages of the reaction. The total number of particles produced also provides information on the energy transfer available from the initial colliding beams to particle production, as a consequence of nuclear stopping [1]. In order to help unravel this complex scenario it is important to compare the particle production amongst collision systems of different sizes over a wide kinematic range.

We present the measured charged-particle pseudorapidity density, $dN_{\text{ch}}/d\eta$, for pp, p–Pb, and Pb–Pb (previously published [2]) collisions at the same collision energy of $\sqrt{s_{\text{NN}}} = 5.02 \text{ TeV}$ in the nucleon–nucleon centre-of-mass reference frame. This is, at present, the maximum available energy at CERN’s Large Hadron Collider (LHC) for Pb–Pb collisions. The measurements were carried out using ALICE at LHC (for earlier $dN_{\text{ch}}/d\eta$ results see for example Refs. [3, 4, 5]). The three studied reactions have different characteristics probing widely different particle production yields and mechanisms. In Pb–Pb collisions, the total particle yield for central collisions is of the order 10^4 [2], and a strongly coupled plasma of quarks and gluons (sQGP) is formed [6, 7, 8, 9], whose collective and transport properties are currently under intense study. On the other hand, pp collisions represent the simplest possible nuclear collision system, where the average total particle production is much smaller (≈ 80 , by integrating the measured distributions), and is to first approximation much less subject to collective effects [10]. The p–Pb system is intermediate to the other reactions, corresponding to the situation where a single nucleon probes the nucleons in a narrow cylinder of the target nucleus. The extent to which p–Pb is governed by the initial state cold nuclear matter of the lead ion or whether collective phenomena in the hot and dense medium play an important role is, at present, a matter under scrutiny by the community [10, 11].

In this letter, we compare the three reactions and present the ratios of the charged-particle pseudorapidity density distributions ($dN_{\text{ch}}/d\eta$) of the more complex reactions to the pp distribution. Owing to ALICE’s unique large acceptance in pseudorapidity, and using simple and robust assumptions, we transform the measured charged-particle pseudorapidity density distributions into charged-particle rapidity density distributions (dN_{ch}/dy). This allows us to calculate the width of the rapidity distributions as a function of the number of participating nucleons. The parameters of the transformation also allow us to estimate a lower bound on the energy density using the well-known formula from Bjorken [12]. An energy density exceeding the critical energy density of roughly 1 GeV/fm^3 [13] is a necessary condition for the formation of deconfined matter of quarks and gluons, and thus it is of the utmost interest to understand the development of these energy densities across different collision systems.

2 Experimental set-up, data sample, analysis method, systematic uncertainties

A detailed description of the ALICE detector and its performance can be found elsewhere [14, 15]. The present analysis uses the Silicon Pixel Detector (SPD) to determine the pseudorapidity densities in the range $-2 < \eta < 2$ and the Forward Multiplicity Detector (FMD) in the ranges $-3.5 < \eta < -1.8$ and $1.8 < \eta < 5$. The V0, comprised of two plastic scintillator discs covering $-3.7 < \eta < -1.7$ (V0C) and $2.8 < \eta < 5.1$ (V0A), and the ZDC, two zero-degree calorimeters located 112.5 m from the interaction point, measurements determine the collision centrality and are used for offline event selection [2].

The results presented are based on data from collisions at a centre-of-mass energy per nucleon pair of $\sqrt{s_{\text{NN}}} = 5.02 \text{ TeV}$ as collected by ALICE during LHC Run 1 (2013) for p–Pb, and during Run 2 (2015) for pp and Pb–Pb. The FMD suffered high levels of background noise during the 2016 p–Pb campaign, due to the high collision rate, and this data is therefore not used for the present analysis. About 10^5 events with a minimum bias trigger requirement [2] were analysed in the centrality range from 0% to 90% and

0% to 100% of the visible cross section for Pb–Pb and p–Pb collisions, respectively. The minimum bias trigger for p–Pb and Pb–Pb collisions in ALICE was defined as a coincidence between the V0A and V0C sides of the V0 detector.

The data from the p–Pb collisions were taken in two beam configurations: one where the lead ion travelled toward positive pseudorapidity and one where it travelled toward negative pseudorapidity. The results from the latter collisions are mirrored around $\eta = 0$. The centre-of-mass frame in p–Pb collisions does not coincide with the laboratory frame, due to the single magnetic field in the LHC, and thus the rapidity of the centre-of-mass is $y_{\text{CM}} = \pm 0.465$ for the two directions, respectively, in the laboratory frame. For this reason, pseudorapidity, calculated with respect to the laboratory frame, is denoted η_{lab} whenever p–Pb results are presented.

Likewise, for the pp collisions, about 10^5 events with coincidence between V0A and V0C and at least one charged particle in $|\eta| < 1$ were analysed. By requiring at least one charged particle at midrapidity, the so-called INEL>0 event class, the systematic uncertainty, related to the absolute normalisation to the full inelastic cross section, is reduced, while still sampling a large fraction ($> 75\%$) of the hadronic cross section [16, 17].

The standard ALICE event selection [18] and centrality estimator based on the V0 amplitude [19, 20] are used in this analysis. The event selection consists of: a) exclusion of background events using the timing information from the ZDC (for Pb–Pb and p–Pb, e.g., beam–gas interactions) and V0 detectors, b) verification of the trigger conditions, and c) a reconstructed position of the collision (primary vertex). In Pb–Pb collisions, centrality is obtained from the sum amplitude in both V0 detector arrays (V0M). For p–Pb only the amplitude in the array on the lead-going side (V0A or V0C) is used. In Pb–Pb collisions, the 10% most peripheral collisions have substantial contributions from electromagnetic processes and are therefore not included in the results presented here [19].

A primary charged particle is defined as a charged particle with a mean proper lifetime τ larger than $1 \text{ cm}/c$, which is either a) produced directly in the interaction, or b) from decays of particles with τ smaller than $1 \text{ cm}/c$ [21]. All quantities reported here are for primary, charged particles, though “primary” is omitted in the following for brevity.

The analysis method is identical to that of previous publications [2]: the measurement of the charged-particle pseudorapidity density at midrapidity is obtained from counting particle trajectories determined using the two layers of the SPD. The SPD has a lower transverse momentum acceptance of $50 \text{ MeV}/c$, and the yield is extrapolated down to $p_{\text{T}} = 0 \text{ MeV}/c$ via simulations. In the forward regions, the measurement is provided by the analysis of the deposited energy signal in the FMD and a statistical method is employed to calculate the inclusive number of charged particles. A data-driven correction [22], based on separate measurements exploiting displaced collision vertices, is applied to remove the background from secondary particles.

Systematic uncertainty estimations for the midrapidity measurements are detailed elsewhere [2, 16, 20], and are from background suppression, transverse momentum extrapolation, weak decays, and simulations. The estimates are obtained through variation of thresholds and simulation studies. For pp (p–Pb), the total systematic uncertainty amounts to 1.5% (2.7%) over the whole pseudorapidity range; while for Pb–Pb the total systematic uncertainty is 2.6% at $\eta = 0$ and 2.9% at $|\eta| = 2$. The systematic uncertainty is mostly correlated over pseudorapidity for $|\eta| < 2$, and largely independent of centrality. The uncertainty in the forward region, estimated via variations of thresholds and simulation studies, is the same for all collision systems and is uncorrelated across η , amounting to 6.9% for $\eta > 3.5$ and 6.4% elsewhere within the forward regions [22]. In the figures of this letter, uncorrelated, local in pseudorapidity, systematic uncertainties are indicated by open boxes on the data points, while correlated systematic uncertainties, those that affect the overall scale and typically from event classification and selection, are indicated by filled boxes to the right of the data. The systematic uncertainty on $dN_{\text{ch}}/d\eta$, due to the

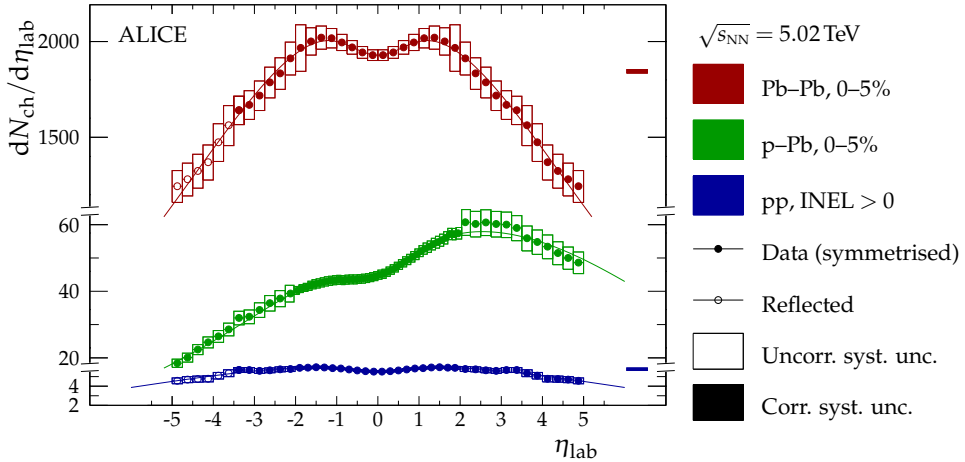


Figure 1: Charged-particle pseudorapidity density in Pb–Pb [2] and p–Pb for the 5% most central collisions, and for pp collisions with $\text{INEL} > 0$ trigger class. For symmetric collision systems (Pb–Pb and pp) the data has been symmetrised around $\eta = 0$ and points for $\eta > 3.5$ have been reflected around $\eta = 0$. The boxes around the points and to the right reflect the uncorrelated and correlated, with respect to pseudorapidity, systematic uncertainty, respectively. The relative correlated, normalisation, uncertainties are evaluated at $dN_{\text{ch}}/d\eta|_{\eta=0}$. The lines show fits of Eq. (1) (Pb–Pb and pp) and Eq. (2) (p–Pb) to the data (discussed in Section 4). Please note that the ordinate has been cut twice to accommodate for the very different ranges of the charged-particle pseudorapidity densities.

centrality class definition in Pb–Pb, is estimated to vary from 0.6% for the most central to 9.5% for the most peripheral class [23]. The 80% to 90% centrality class has residual contamination from electromagnetic processes as detailed elsewhere [19], which gives rise to an additional 4% systematic uncertainty in the measurements. No overall systematic uncertainty has been estimated for p–Pb collisions, as the centrality selection in that collision system is inherently difficult to map to the underlying dynamics of the collisions [20].

3 Results

Figure 1 shows the measured pseudorapidity densities in pp, and in central p–Pb, and the previously published results for Pb–Pb [2] collisions at $\sqrt{s_{\text{NN}}} = 5.02 \text{ TeV}$ for primary particles.

For the 5% most central Pb–Pb collisions $dN_{\text{ch}}/d\eta \approx 2000$ at midrapidity ($\eta = 0$) [2], while for p–Pb collisions the distribution peaks at $dN_{\text{ch}}/d\eta_{\text{lab}} \approx 60$ around $\eta_{\text{lab}} = 3$ in the lead-going direction ($\eta > 0$). For pp collisions with the $\text{INEL} > 0$ trigger condition discussed above, $dN_{\text{ch}}/d\eta = 5.7 \pm 0.2$ at midrapidity, consistent with previous results derived from p_T spectra [24].

Figure 2 shows, as a function of centrality, the measured charged-particle pseudorapidity densities for p–Pb collisions at $\sqrt{s_{\text{NN}}} = 5.02 \text{ TeV}$. The strategy of centrality selection for proton on nucleus reactions is explained elsewhere [20]. The ALICE Collaboration has previously presented $dN_{\text{ch}}/d\eta$ for Pb–Pb collisions at this energy [2].

In Fig. 3, the charged-particle pseudorapidity densities in p–Pb and Pb–Pb reactions are divided by the pp distributions corresponding to the $\text{INEL} > 0$ trigger class. The ratio is $r_X = (dN_{\text{ch}}/d\eta|_X)/(dN_{\text{ch}}/d\eta|_{\text{pp}})$, where X labels p–Pb and Pb–Pb collisions, in centrality classes, as a function of pseudorapidity. In the ratios, systematic uncertainties, of common origin, are partially cancelled, and, as an estimate, the magnitude of the resulting systematic uncertainties are given only by the uncertainties in the $dN_{\text{ch}}/d\eta|_X$ measurements, since the uncertainties are independent of the collision system. In p–Pb collisions the rapidity of the centre-of-mass is non-zero, which is not taken into account in the ratios. Such a correction would require prior determination of the full Jacobian of the transformation from pseudorapidity to

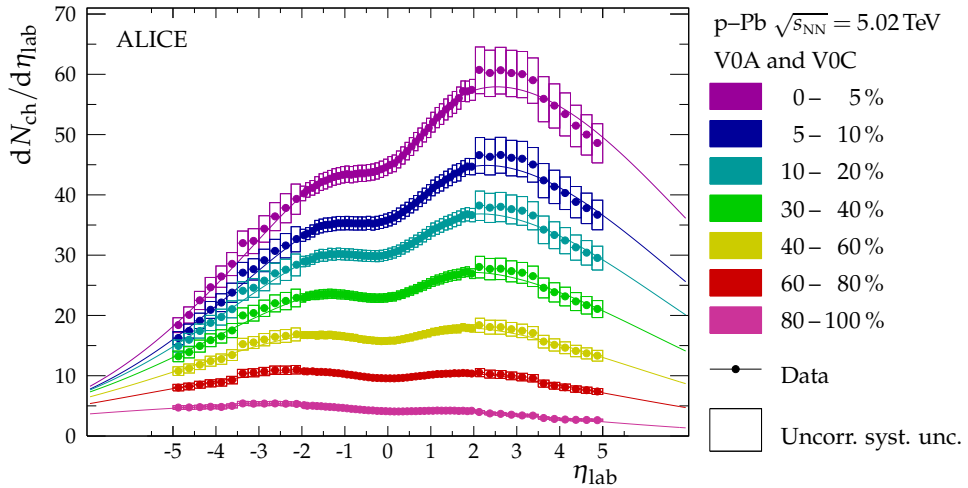


Figure 2: Charged-particle pseudorapidity density in p–Pb collisions at $\sqrt{s_{\text{NN}}} = 5.02 \text{ TeV}$ in seven centrality classes based on the V0A and V0C estimators. The lines are obtained using a fit of a scaled, normal distribution in rapidity Eq. (2) to the data (discussed in Section 4).

rapidity, which is not possible to perform reliably with the ALICE apparatus.

The ratio of the p–Pb relative to the pp distributions increases with pseudorapidity from the p-going to the Pb-going direction for central collisions, which Brodsky *et al* and Adil *et al* [25, 26] suggest is a sign of scaling of the pp distribution with the increasing number of participants as the lead nucleus is probed by the incident proton, and thus independent proton–nucleon scatterings on the lead-ion side. A similar scaling, however, does not hold for the Pb–Pb reaction. The ratios cannot be obtained by simple scaling of the elementary pp distributions. Instead, the ratio of the Pb–Pb relative to the pp distributions exhibits an enhancement of particle production around midrapidity for the more central collisions which is indicative of the formation of the sQGP [7]. Likewise, r_{pPb} increases for all but the two most peripheral centrality classes as $\eta_{\text{lab}} \rightarrow 3$. In Pb–Pb collisions it is seen that the various mechanisms behind the pseudorapidity distributions are more transversely directed than in pp collisions by the increase of r_{pPb} as $|\eta| \rightarrow 0$.

4 Rapidity and energy-density dependence on system size and discussion

It has been shown that the charged-particle *rapidity* density (dN_{ch}/dy) in Pb–Pb collisions, to a good accuracy, follows a normal distribution over the considered rapidity interval ($|y| \lesssim 5$) [2, 27]. Those results relied on calculating the average Jacobian $dN_{\text{ch}}/dy = \langle J \rangle = \langle \beta \rangle$ using the full p_{T} spectra, at midrapidity, of charged pions and kaons as well as protons and antiprotons. Here, we use the approximation

$$y \approx \eta - \frac{1}{2} \frac{m^2}{p_{\text{T}}^2} \cos \vartheta,$$

where ϑ is the polar angle of emission, and identify $a = p_{\text{T}}/m$ with an effective ratio of transverse momentum over mass. With this, the effective Jacobian can be written as

$$J'(\eta, a) = \left(1 + \frac{1}{a^2} \frac{1}{\cosh^2 \eta} \right)^{-1/2}.$$

We further make the ansatz that dN_{ch}/dy is normal distributed for symmetric collision systems (pp and Pb–Pb), so that $dN_{\text{ch}}/d\eta$ can be parameterised as

$$f(\eta; A, a, \sigma) = J'(\eta, a) A \frac{1}{\sqrt{2\pi}\sigma} \exp \left(-\frac{\eta^2 - \langle \eta, a \rangle}{2\sigma^2} \right), \quad (1)$$

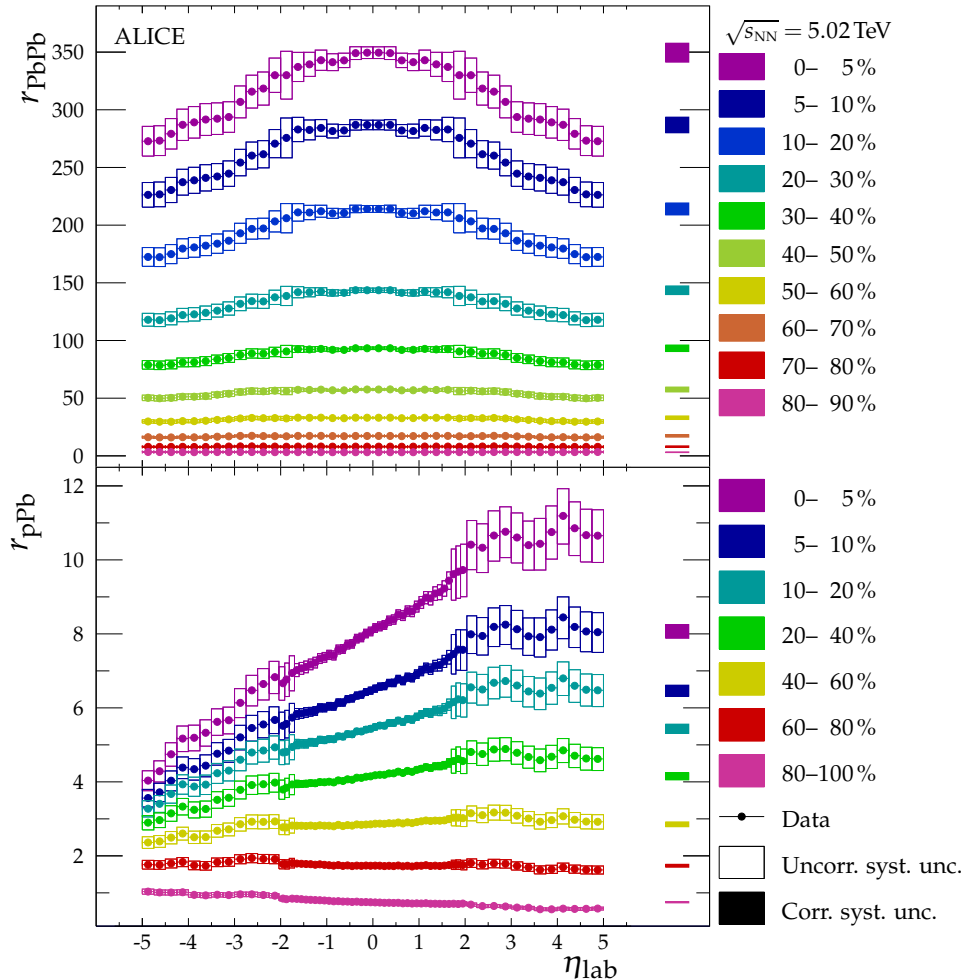


Figure 3: Ratio r_X of the charged-particle pseudorapidity density in Pb–Pb (top) and p–Pb (bottom) in different centrality classes to the charged-particle pseudorapidity density in pp in the INEL>0 event class. Note, for Pb–Pb η_{lab} is the same as the centre-of-mass pseudorapidity.

where A and σ are the total integral and width of the distribution, respectively, and y the rapidity in the centre-of-mass frame. Motivated by the observed approximate linearity of r_{pPb} (see lower panel of Fig. 3), we replace A with $(\alpha y + A)$ for the asymmetric system (p–Pb) and parameterise $dN_{\text{ch}}/d\eta_{\text{lab}}$ as

$$g(\eta; A, a, \alpha, \sigma) = J'(\eta, a) (\alpha y\{\eta, a\} + A) \frac{1}{\sqrt{2\pi}\sigma} \exp\left(-\frac{[y\{\eta, a\} - y_{\text{CM}}]^2}{2\sigma^2}\right). \quad (2)$$

The functions f and g defined in Eq. (1) and Eq. (2), respectively, describe the measurements within the measured region with χ^2 per degrees of freedom (v) in the range of 0.1 to 0.5. The small χ^2/v values are a consequence of the relatively large uncorrelated systematic uncertainties on the measurements. That is, the charged-particle distributions for pp, p–Pb, and Pb–Pb collisions at $\sqrt{s_{\text{NN}}} = 5.02 \text{ TeV}$ follow a normal distribution in rapidity, with free parameters A , a , σ , and α in the asymmetric case.

The top panel of Fig. 4 shows the best-fit parameter values of the normal width ($\sigma_{dN_{\text{ch}}/dy}$) for all three collision systems as a function of the average number of participating nucleons ($\langle N_{\text{part}} \rangle$) calculated using a Glauber model [28]. The best-fit parameters are found taking statistical and uncorrelated systematic uncertainties into account. The result using the above procedure, for the most central Pb–Pb collisions, is found to be compatible with previous results extracted by unfolding with the mean Jacobian estimated from transverse momentum spectra [2]. The open points (crosses) and dashed lines on the figure are from evaluations of Eq. (1) and Eq. (2), and direct calculations of $\sigma_{dN_{\text{ch}}/dy}$, respectively, using model

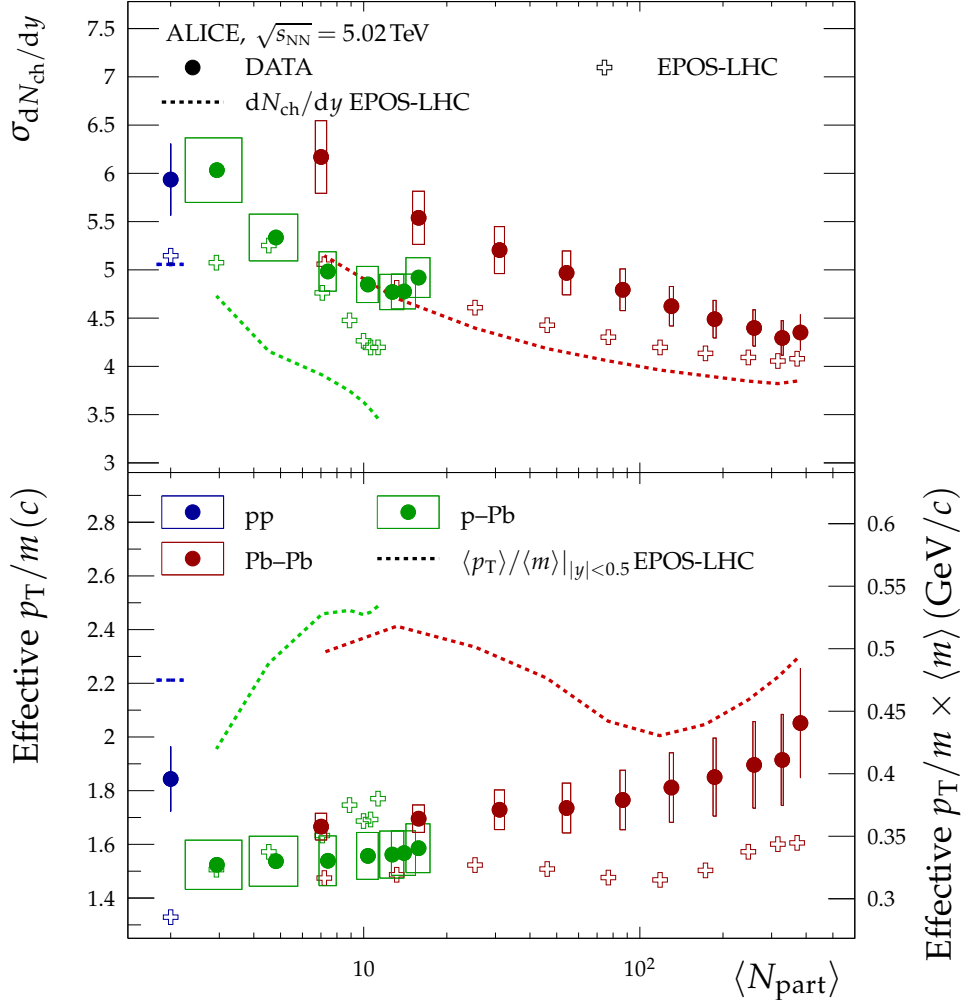


Figure 4: The width (top) and effective p_{T}/m (bottom) fit parameters as a function of the mean number of participants in pp, p–Pb, and Pb–Pb collisions at $\sqrt{s_{\text{NN}}} = 5.02 \text{ TeV}$. Vertical uncertainties are the standard error on the best-fit parameter values, while horizontal uncertainties reflect the uncertainty on $\langle N_{\text{part}} \rangle$ from the Glauber calculations. Also shown are similar fit parameters from the same parameterisation of EPOS-LHC calculations as well as direct calculations of the standard deviation of the dN_{ch}/dy distributions and the $\langle p_{\text{T}} \rangle / \langle m \rangle$ ratio from the EPOS-LHC calculations.

calculations with EPOS-LHC [29]. EPOS-LHC was chosen as it provides predictions for all three collision systems. The parameterisation, in terms of the two functions, of this model calculation generally reproduces the widths of the charged-particle rapidity densities, except in the asymmetric case where a direct evaluation of the standard deviation is less motivated.

The general trend is that the widths decrease as $\langle N_{\text{part}} \rangle$ increases, consistent with the behaviour of the r_{PbPb} ratios. Notably, the width of the dN_{ch}/dy distributions in p–Pb and Pb–Pb, for low number of participant nucleons in the collisions, approaches the width of the pp distribution, which, presumably, is dominated by kinematic and phase space constraints.

The lower panel of Fig. 4 shows the dependence of a on the average number of participants. The right-hand ordinate is the same, but multiplied by the average mass $\langle m \rangle = (0.215 \pm 0.001) \text{ GeV}/c^2$ estimated from measurements of identified particles in Pb–Pb collisions at $\sqrt{s_{\text{NN}}} = 2.76 \text{ TeV}$ [30]. To better understand the parameter a , this parameter extracted from the EPOS-LHC calculations, using the above procedure, is also shown in the figure. The dotted lines show the average p_{T}/m predicted by EPOS-

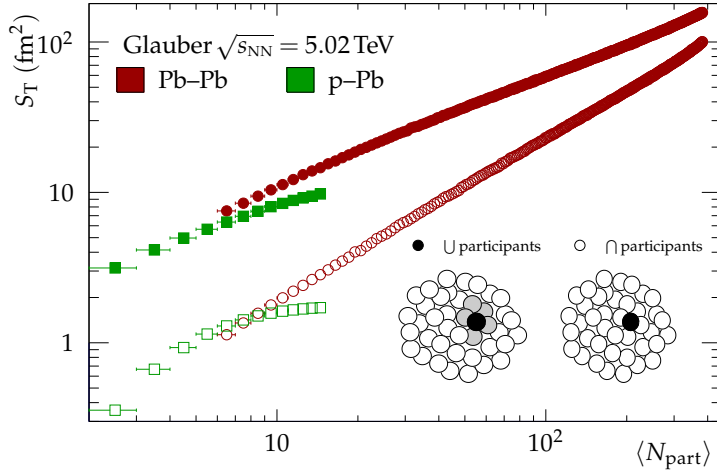


Figure 5: The transverse area S_T as calculated in a numerical Glauber model for two extreme cases: a) only the exclusive overlap of nucleons is considered (\cap , open markers) and b) the inclusive area of participating nucleons contribute (\cup , closed markers) in both p–Pb and Pb–Pb at $\sqrt{s_{\text{NN}}} = 5.02 \text{ TeV}$.

LHC [29]. The EPOS-LHC calculations indicate that the extracted effective transverse momentum to mass ratio a is consistently smaller than the ratio of the average transverse momentum to the average mass. Thus a gives a lower bound on $\langle p_{\text{T}} \rangle / \langle m \rangle$.

We can estimate the energy density that is reached in the collisions as a function of the number of participants for the three systems. A conventional approach is to use the model originally proposed by Bjorken [12] in which the energy density (ε_{Bj}) depends on the rapidity density of particles and the volume of a longitudinal cylinder with cross sectional area determined by the overlap between the colliding partners and length determined by a characteristic particle formation time

$$\varepsilon_{\text{Bj}} = \frac{1}{c\tau} \frac{1}{S_T} \left\langle \frac{dE_{\text{T}}}{dy} \right\rangle.$$

Here, $S_T \approx \pi R^2 \approx \pi N_{\text{part}}^{2/3}$ is the transverse area spanned by the participating nucleons, dE_{T}/dy is the transverse-energy rapidity density, and τ is the formation time. While a formation time of $\tau = 1 \text{ fm}/c$ is often assumed, it is left as a free parameter here. With $\langle m_{\text{T}} \rangle = \langle m \rangle \sqrt{1 + (\langle p_{\text{T}} \rangle / \langle m \rangle)^2}$, the transverse-energy rapidity density can be approximated by

$$\left\langle \frac{dE_{\text{T}}}{dy} \right\rangle \approx \langle m_{\text{T}} \rangle \frac{1}{f_{\text{total}}} \frac{dN_{\text{ch}}}{dy} = \langle m \rangle \sqrt{1 + \left(\frac{\langle p_{\text{T}} \rangle}{\langle m \rangle} \right)^2} \frac{1}{f_{\text{total}}} \frac{dN_{\text{ch}}}{dy},$$

where $f_{\text{total}} = 0.55 \pm 0.01$, the ratio of charged particles to all particles [31], accounts for neutral particles not measured in the experiment, and is assumed the same for all collision systems. Substituting the derived dN_{ch}/dy and the effective $a = p_{\text{T}}/m \lesssim \langle p_{\text{T}} \rangle / \langle m \rangle$ results in a lower bound estimate for the Bjorken energy density (ε_{LB})

$$\varepsilon_{\text{Bj}} \tau \geq \varepsilon_{\text{LB}} \tau = \frac{1}{c} \frac{1}{S_T} \langle m \rangle \sqrt{1 + a^2} \frac{1}{f_{\text{total}}} \sqrt{1 + \frac{1}{a^2} \frac{1}{\cosh^2 \eta}} \frac{dN_{\text{ch}}}{dy}, \quad (3)$$

where a and $\langle m \rangle$ are as in the top panel of Fig. 4.

The transverse area S_T is estimated in a numerical Glauber model [32, 33] as shown in Fig. 5. We consider two extremes for the transverse area spanned by the participating nucleons: a) the *exclusive* (or direct) overlap between participating nucleons, \cap and open markers in Fig. 5, and b) the *inclusive* (or full) area of all participating nucleons, \cup and full markers in Fig. 5.

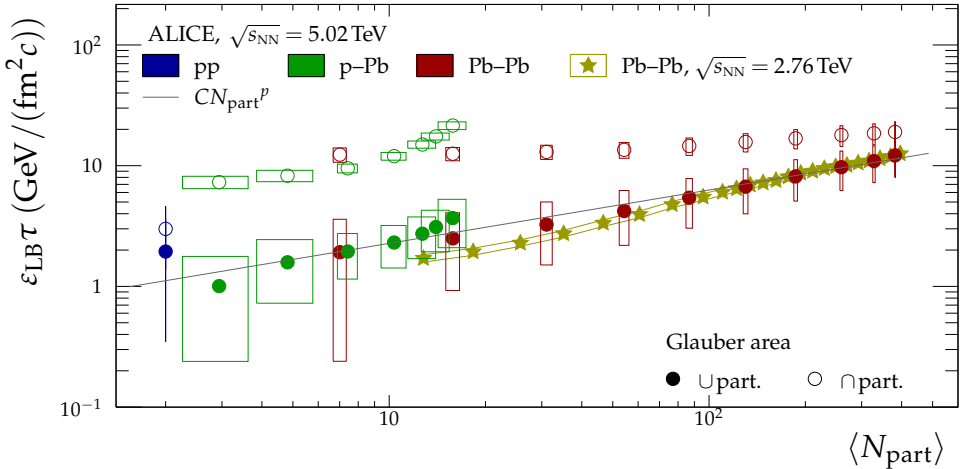


Figure 6: Estimate of the lower bound on the Bjorken transverse energy density in pp, p–Pb, and Pb–Pb collisions at $\sqrt{s_{\text{NN}}} = 5.02 \text{ TeV}$, considering the exclusive (\cap , open markers) and inclusive (\cup , full markers) overlap area S_T of the nucleons. The expression CN_{part}^p is fitted to case \cup , and we find $C = (0.8 \pm 0.3) \text{ GeV}/(\text{fm}^2 c)$ and $p = 0.44 \pm 0.08$. Also shown is an estimate, via dE_T/dy , of ε_{Bj} from Pb–Pb collisions at $\sqrt{s_{\text{NN}}} = 2.76 \text{ TeV}$ (stars with uncertainty band) [31].

Figure 6 shows the lower-bound energy density estimate, $\varepsilon_{\text{LB}}\tau \leq \varepsilon_{\text{Bj}}\tau$, as a function of the number of participants, which reaches values between 10 and $20 \text{ GeV}/(\text{fm}^2 c)$ in the most central Pb–Pb collisions. The uncertainties are from standard error propagation of Eq. (3) of uncertainties on the best-fit parameter values, the number of participants, mean mass, and f_{total} . A rise from roughly $1 \text{ GeV}/(\text{fm}^2 c)$ to over $10 \text{ GeV}/(\text{fm}^2 c)$ is observed if the transverse area is assumed to be the inclusive area of participating nucleons. This trend is illustrated by a power-law (CN_{part}^p) fit to the data in the figure, with the parameter values $C = (0.8 \pm 0.3) \text{ GeV}/(\text{fm}^2 c)$ and $p = 0.44 \pm 0.08$. On the other hand, if the transverse area is assumed to be the smaller exclusive overlap area, we observe a substantially larger lower bound on the energy density, but a less dramatic increase with increasing number of participating nucleons. Also shown in the figure are estimates of the Bjorken energy density $\varepsilon_{\text{Bj}}\tau$ for Pb–Pb reactions at $\sqrt{s_{\text{NN}}} = 2.76 \text{ TeV}$ [31]. These results were obtained from measurements of the transverse energy in the collisions and using the inclusive estimate of the transverse area S_T . The trend of the $\sqrt{s_{\text{NN}}} = 5.02 \text{ TeV}$ results are similar to these earlier results. Bearing in mind that for the largest LHC collision energy we show a lower bound estimate of the energy density in Fig. 6, we find a likely overall increase in the energy density from $\sqrt{s_{\text{NN}}} = 2.76 \text{ TeV}$ to 5.02 TeV .

5 Summary and conclusions

We have measured the charged particle pseudorapidity density in pp, p–Pb, and Pb–Pb collisions at $\sqrt{s_{\text{NN}}} = 5.02 \text{ TeV}$ over the widest possible pseudorapidity range available at the LHC. The distributions were determined using the same experimental apparatus and methods, and systematic uncertainties have been minimised to within the capabilities of the set-up. While the particle production in central Pb–Pb collisions clearly exhibits an enhancement as compared to pp collisions, particle production in p–Pb collisions is consistent with dominantly incoherent nucleon–nucleon collisions. By transforming the measured pseudorapidity distributions to rapidity distributions we have obtained systematic trends for the width of the rapidity distributions and a lower bound on the energy density, which shows a clear scaling behaviour as a function of the average number of participant nucleons. The decreasing width of the deduced rapidity distributions with increasing participant number suggests that the kinematic spread of particles, including longitudinal degrees of freedom, is reduced due to interactions in the early stages of the collisions. This is also reflected in the accompanying growth of the energy density. Both observations

are consistent with the gradual establishment of a high-density phase of matter with increasing size of the collision domain.

Acknowledgements

The ALICE Collaboration would like to thank all its engineers and technicians for their invaluable contributions to the construction of the experiment and the CERN accelerator teams for the outstanding performance of the LHC complex. The ALICE Collaboration gratefully acknowledges the resources and support provided by all Grid centres and the Worldwide LHC Computing Grid (WLCG) collaboration. The ALICE Collaboration acknowledges the following funding agencies for their support in building and running the ALICE detector: A. I. Alikhanyan National Science Laboratory (Yerevan Physics Institute) Foundation (ANSL), State Committee of Science and World Federation of Scientists (WFS), Armenia; Austrian Academy of Sciences, Austrian Science Fund (FWF): [M 2467-N36] and Nationalstiftung für Forschung, Technologie und Entwicklung, Austria; Ministry of Communications and High Technologies, National Nuclear Research Center, Azerbaijan; Conselho Nacional de Desenvolvimento Científico e Tecnológico (CNPq), Financiadora de Estudos e Projetos (Finep), Fundação de Amparo à Pesquisa do Estado de São Paulo (FAPESP) and Universidade Federal do Rio Grande do Sul (UFRGS), Brazil; Ministry of Education of China (MOEC) , Ministry of Science & Technology of China (MSTC) and National Natural Science Foundation of China (NSFC), China; Ministry of Science and Education and Croatian Science Foundation, Croatia; Centro de Aplicaciones Tecnológicas y Desarrollo Nuclear (CEADEN), Cubaenergía, Cuba; Ministry of Education, Youth and Sports of the Czech Republic, Czech Republic; The Danish Council for Independent Research | Natural Sciences, the VILLUM FONDEN and Danish National Research Foundation (DNRF), Denmark; Helsinki Institute of Physics (HIP), Finland; Commissariat à l’Energie Atomique (CEA) and Institut National de Physique Nucléaire et de Physique des Particules (IN2P3) and Centre National de la Recherche Scientifique (CNRS), France; Bundesministerium für Bildung und Forschung (BMBF) and GSI Helmholtzzentrum für Schwerionenforschung GmbH, Germany; General Secretariat for Research and Technology, Ministry of Education, Research and Religions, Greece; National Research, Development and Innovation Office, Hungary; Department of Atomic Energy Government of India (DAE), Department of Science and Technology, Government of India (DST), University Grants Commission, Government of India (UGC) and Council of Scientific and Industrial Research (CSIR), India; National Research and Innovation Agency - BRIN, Indonesia; Istituto Nazionale di Fisica Nucleare (INFN), Italy; Japanese Ministry of Education, Culture, Sports, Science and Technology (MEXT) and Japan Society for the Promotion of Science (JSPS) KAKENHI, Japan; Consejo Nacional de Ciencia (CONACYT) y Tecnología, through Fondo de Cooperación Internacional en Ciencia y Tecnología (FONCICYT) and Dirección General de Asuntos del Personal Académico (DGAPA), Mexico; Nederlandse Organisatie voor Wetenschappelijk Onderzoek (NWO), Netherlands; The Research Council of Norway, Norway; Commission on Science and Technology for Sustainable Development in the South (COMSATS), Pakistan; Pontificia Universidad Católica del Perú, Peru; Ministry of Education and Science, National Science Centre and WUT ID-UB, Poland; Korea Institute of Science and Technology Information and National Research Foundation of Korea (NRF), Republic of Korea; Ministry of Education and Scientific Research, Institute of Atomic Physics, Ministry of Research and Innovation and Institute of Atomic Physics and University Politehnica of Bucharest, Romania; Ministry of Education, Science, Research and Sport of the Slovak Republic, Slovakia; National Research Foundation of South Africa, South Africa; Swedish Research Council (VR) and Knut & Alice Wallenberg Foundation (KAW), Sweden; European Organization for Nuclear Research, Switzerland; Suranaree University of Technology (SUT), National Science and Technology Development Agency (NSTDA), Thailand Science Research and Innovation (TSRI) and National Science, Research and Innovation Fund (NSRF), Thailand; Turkish Energy, Nuclear and Mineral Research Agency (TENMAK), Turkey; National Academy of Sciences of Ukraine, Ukraine; Science and Technology Facilities Council (STFC), United Kingdom; National Science Foundation of the United States of America (NSF) and United States Department of Energy, Office

of Nuclear Physics (DOE NP), United States of America. In addition, individual groups or members have received support from: Marie Skłodowska Curie, Strong 2020 - Horizon 2020 (grant nos. 824093, 896850), European Union; Academy of Finland (Center of Excellence in Quark Matter) (grant nos. 346327, 346328), Finland.

References

- [1] **BRAHMS** Collaboration, I. C. Arsene *et al.*, “Nuclear stopping and rapidity loss in Au+Au collisions at $\sqrt{s_{\text{NN}}} = 62.4 \text{ GeV}$ ”, *Phys. Lett.* **B677** (2009) 267–271, arXiv:0901.0872 [nucl-ex].
- [2] **ALICE** Collaboration, J. Adam *et al.*, “Centrality dependence of the pseudorapidity density distribution for charged particles in Pb–Pb collisions at $\sqrt{s_{\text{NN}}} = 5.02 \text{ TeV}$ ”, *Phys. Lett.* **B772** (2017) 567–577, arXiv:1612.08966 [nucl-ex].
- [3] **NA50** Collaboration, M. C. Abreu *et al.*, “Scaling of charged particle multiplicity in Pb-Pb collisions at SPS energies”, *Phys. Lett.* **B530** (2002) 43–55.
- [4] **PHOBOS** Collaboration, B. Alver *et al.*, “Charged-particle multiplicity and pseudorapidity distributions measured with the PHOBOS detector in Au+Au, Cu+Cu, d+Au, p+p collisions at ultrarelativistic energies”, *Phys. Rev.* **C83** (2011) 024913, arXiv:1011.1940 [nucl-ex].
- [5] **ATLAS** Collaboration, G. Aad *et al.*, “Measurement of the centrality dependence of the charged-particle pseudorapidity distribution in proton–lead collisions at $\sqrt{s_{\text{NN}}} = 5.02 \text{ TeV}$ with the ATLAS detector”, *Eur. Phys. J.* **C76** (2016) 199, arXiv:1508.00848 [hep-ex].
- [6] **BRAHMS** Collaboration, I. Arsene *et al.*, “Quark gluon plasma and color glass condensate at RHIC? The Perspective from the BRAHMS experiment”, *Nucl. Phys.* **A757** (2005) 1–27, arXiv:nucl-ex/0410020 [nucl-ex].
- [7] **PHOBOS** Collaboration, B. B. Back *et al.*, “The PHOBOS perspective on discoveries at RHIC”, *Nucl. Phys.* **A757** (2005) 28–101, arXiv:nucl-ex/0410022 [nucl-ex].
- [8] **STAR** Collaboration, J. Adams *et al.*, “Experimental and theoretical challenges in the search for the quark gluon plasma: The STAR Collaboration’s critical assessment of the evidence from RHIC collisions”, *Nucl. Phys.* **A757** (2005) 102–183, arXiv:nucl-ex/0501009 [nucl-ex].
- [9] **PHENIX** Collaboration, K. Adcox *et al.*, “Formation of dense partonic matter in relativistic nucleus-nucleus collisions at RHIC: Experimental evaluation by the PHENIX collaboration”, *Nucl. Phys.* **A757** (2005) 184–283, arXiv:nucl-ex/0410003 [nucl-ex].
- [10] C. Bierlich, T. Sjöstrand, and M. Utheim, “Hadronic rescattering in pA and AA collisions”, *Eur. Phys. J.* **A57** (2021) 227, arXiv:2103.09665 [hep-ph].
- [11] Z.-W. Lin and L. Zheng, “Further developments of a multi-phase transport model for relativistic nuclear collisions”, *Nucl. Sci. Tech.* **32** (2021) 113, arXiv:2110.02989 [nucl-th].
- [12] J. D. Bjorken, “Highly relativistic nucleus-nucleus collisions: The central rapidity region”, *Phys. Rev.* **D27** (Jan, 1983) 140–151.
- [13] H.-T. Ding, “Recent lattice QCD results and phase diagram of strongly interacting matter”, *Nucl. Phys.* **A931** (2014) 52–62, arXiv:1408.5236 [hep-lat].
- [14] **ALICE** Collaboration, K. Aamodt *et al.*, “The ALICE experiment at the CERN LHC”, *JINST* **3** (2008) S08002.
- [15] **ALICE** Collaboration, B. Abelev *et al.*, “Performance of the ALICE Experiment at the CERN LHC”, *Int. J. Mod. Phys.* **A29** (2014) 1430044, arXiv:1402.4476 [nucl-ex].
- [16] **ALICE** Collaboration, J. Adam *et al.*, “Charged-particle multiplicities in proton–proton collisions at $\sqrt{s} = 0.9$ to 8 TeV”, *Eur. Phys. J.* **C77** (2017) 33, arXiv:1509.07541 [nucl-ex].
- [17] **ALICE** Collaboration, S. Acharya *et al.*, “Pseudorapidity distributions of charged particles as a function of mid- and forward rapidity multiplicities in pp collisions at $\sqrt{s} = 5.02, 7$ and 13 TeV”,

- Eur. Phys. J.* **C81** (2021) 630, arXiv:2009.09434 [nucl-ex].
- [18] ALICE Collaboration, K. Aamodt *et al.*, “Charged-particle multiplicity density at mid-rapidity in central Pb–Pb collisions at $\sqrt{s_{\text{NN}}} = 2.76 \text{ TeV}$ ”, *Phys. Rev. Lett.* **105** (2010) 252301, arXiv:1011.3916 [nucl-ex].
- [19] ALICE Collaboration, B. Abelev *et al.*, “Centrality determination of Pb-Pb collisions at $\sqrt{s_{\text{NN}}} = 2.76 \text{ TeV}$ with ALICE”, *Phys. Rev.* **C88** (2013) 044909, arXiv:1301.4361 [nucl-ex].
- [20] ALICE Collaboration, J. Adam *et al.*, “Centrality dependence of particle production in p-Pb collisions at $\sqrt{s_{\text{NN}}} = 5.02 \text{ TeV}$ ”, *Phys. Rev.* **C91** (2015) 064905, arXiv:1412.6828 [nucl-ex].
- [21] ALICE Collaboration, S. Acharya *et al.*, “The ALICE definition of primary particles”, ALICE-PUBLIC-2017-005. <https://cds.cern.ch/record/2270008>.
- [22] ALICE Collaboration, J. Adam *et al.*, “Centrality evolution of the charged-particle pseudorapidity density over a broad pseudorapidity range in Pb-Pb collisions at $\sqrt{s_{\text{NN}}} = 2.76 \text{ TeV}$ ”, *Phys. Lett.* **B754** (2016) 373–385, arXiv:1509.07299 [nucl-ex].
- [23] ALICE Collaboration, J. Adam *et al.*, “Centrality dependence of the charged-particle multiplicity density at midrapidity in Pb-Pb collisions at $\sqrt{s_{\text{NN}}} = 5.02 \text{ TeV}$ ”, *Phys. Rev. Lett.* **116** (2016) 222302, arXiv:1512.06104 [nucl-ex].
- [24] ALICE Collaboration, S. Acharya *et al.*, “Charged-particle production as a function of multiplicity and transverse spherocity in pp collisions at $\sqrt{s} = 5.02$ and 13 TeV ”, *Eur. Phys. J.* **C79** (2019) 857, arXiv:1905.07208 [nucl-ex].
- [25] S. J. Brodsky *et al.*, “Hadron Production in Nuclear Collisions: A New Parton Model Approach”, *Phys. Rev. Lett.* **39** (1977) 1120.
- [26] A. Adil *et al.*, “3D jet tomography of twisted strongly coupled quark gluon plasmas”, *Phys. Rev.* **C72** (2005) 034907, arXiv:nucl-th/0505004 [nucl-th].
- [27] ALICE Collaboration, E. Abbas *et al.*, “Centrality dependence of the pseudorapidity density distribution for charged particles in Pb–Pb collisions at $\sqrt{s_{\text{NN}}} = 2.76 \text{ TeV}$ ”, *Phys. Lett.* **B726** (2013) 610–622, arXiv:1304.0347 [nucl-ex].
- [28] ALICE Collaboration, S. Acharya *et al.*, “Centrality determination in heavy ion collisions”, ALICE-PUBLIC-2018-011. <http://cds.cern.ch/record/2636623>.
- [29] T. Pierog *et al.*, “EPOS LHC: Test of collective hadronization with data measured at the CERN Large Hadron Collider”, *Phys. Rev.* **C92** (2015) 034906, arXiv:1306.0121 [hep-ph].
- [30] ALICE Collaboration, B. Abelev *et al.*, “Centrality dependence of π , K, p production in Pb-Pb collisions at $\sqrt{s_{\text{NN}}} = 2.76 \text{ TeV}$ ”, *Phys. Rev.* **C88** (2013) 044910, arXiv:1303.0737 [hep-ex].
- [31] ALICE Collaboration, J. Adam *et al.*, “Measurement of transverse energy at midrapidity in Pb–Pb collisions at $\sqrt{s_{\text{NN}}} = 2.76 \text{ TeV}$ ”, *Phys. Rev.* **C94** (2016) 034903, arXiv:1603.04775 [nucl-ex].
- [32] C. Loizides, J. Nagle, and P. Steinberg, “Improved version of the PHOBOS Glauber Monte Carlo”, *SoftwareX* **1-2** (2015) 13 – 18.
- [33] C. Loizides, “Glauber modeling of high-energy nuclear collisions at the subnucleon level”, *Phys. Rev.* **C94** (2016) 024914, arXiv:1603.07375 [nucl-ex].

A The ALICE Collaboration

- S. Acharya ^{123,130}, D. Adamová ⁸⁵, A. Adler ⁶⁸, G. Aglieri Rinella ³², M. Agnello ²⁹, N. Agrawal ⁴⁹, Z. Ahammed ¹³⁰, S. Ahmad ¹⁵, S.U. Ahn ⁶⁹, I. Ahuja ³⁶, A. Akindinov ¹³⁸, M. Al-Turany ⁹⁷, D. Aleksandrov ¹³⁸, B. Alessandro ⁵⁴, H.M. Alfanda ⁶, R. Alfaro Molina ⁶⁵, B. Ali ¹⁵, Y. Ali ¹³, A. Alici ²⁵, N. Alizadehvandchali ¹¹², A. Alkin ³², J. Alme ²⁰, G. Alocco ⁵⁰, T. Alt ⁶², I. Altsybeev ¹³⁸, M.N. Anaam ⁶, C. Andrei ⁴⁴, A. Andronic ¹³³, V. Anguelov ⁹⁴, F. Antinori ⁵², P. Antonioli ⁴⁹, C. Anuj ¹⁵, N. Apadula ⁷³, L. Aphecetche ¹⁰², H. Appelshäuser ⁶², S. Arcelli ²⁵, R. Arnaldi ⁵⁴, I.C. Arsene ¹⁹, M. Arslanbekov ¹³⁵, A. Augustinus ³², R. Averbeck ⁹⁷, S. Aziz ⁷¹, M.D. Azmi ¹⁵, A. Badalà ⁵¹, Y.W. Baek ³⁹, X. Bai ⁹⁷, R. Bailhache ⁶², Y. Bailung ⁴⁶, R. Bala ⁹⁰, A. Balbino ²⁹, A. Baldissari ¹²⁶, B. Balis ², D. Banerjee ⁴, Z. Banoo ⁹⁰, R. Barbera ²⁶, L. Barioglio ⁹⁵, M. Barlou ⁷⁷, G.G. Barnaföldi ¹³⁴, L.S. Barnby ⁸⁴, V. Barret ¹²³, L. Barreto ¹⁰⁸, C. Bartels ¹¹⁵, K. Barth ³², E. Bartsch ⁶², F. Baruffaldi ²⁷, N. Bastid ¹²³, S. Basu ⁷⁴, G. Batigne ¹⁰², D. Battistini ⁹⁵, B. Batyunya ¹³⁹, D. Bauri ⁴⁵, J.L. Bazo Alba ¹⁰⁰, I.G. Bearden ⁸², C. Beattie ¹³⁵, P. Becht ⁹⁷, I. Belikov ¹²⁵, A.D.C. Bell Hechavarria ¹³³, R. Bellwied ¹¹², S. Belokurova ¹³⁸, V. Belyaev ¹³⁸, G. Bencedi ^{134,63}, S. Beole ²⁴, A. Bercuci ⁴⁴, Y. Berdnikov ¹³⁸, A. Berdnikova ⁹⁴, L. Bergmann ⁹⁴, M.G. Besoiu ⁶¹, L. Betev ³², P.P. Bhaduri ¹³⁰, A. Bhasin ⁹⁰, I.R. Bhat ⁹⁰, M.A. Bhat ⁴, B. Bhattacharjee ⁴⁰, L. Bianchi ²⁴, N. Bianchi ⁴⁷, J. Bielčík ³⁵, J. Bielčíková ⁸⁵, J. Biernat ¹⁰⁵, A. Bilandzic ⁹⁵, G. Biro ¹³⁴, S. Biswas ⁴, J.T. Blair ¹⁰⁶, D. Blau ¹³⁸, M.B. Blidaru ⁹⁷, N. Bluhme ³⁷, C. Blume ⁶², G. Boca ^{21,53}, F. Bock ⁸⁶, A. Bogdanov ¹³⁸, S. Boi ²², J. Bok ⁵⁶, L. Boldizsár ¹³⁴, A. Bolozdynya ¹³⁸, M. Bombara ³⁶, P.M. Bond ³², G. Bonomi ^{129,53}, H. Borel ¹²⁶, A. Borissov ¹³⁸, H. Bossi ¹³⁵, E. Botta ²⁴, L. Bratrud ⁶², P. Braun-Munzinger ⁹⁷, M. Bregant ¹⁰⁸, M. Broz ³⁵, G.E. Bruno ^{96,31}, M.D. Buckland ¹¹⁵, D. Budnikov ¹³⁸, H. Buesching ⁶², S. Bufalino ²⁹, O. Bugnon ¹⁰², P. Buhler ¹⁰¹, Z. Buthelezi ^{66,119}, J.B. Butt ¹³, A. Bylinkin ¹¹⁴, S.A. Bysiak ¹⁰⁵, M. Cai ^{27,6}, H. Caines ¹³⁵, A. Caliva ⁹⁷, E. Calvo Villar ¹⁰⁰, J.M.M. Camacho ¹⁰⁷, R.S. Camacho ⁴³, P. Camerini ²³, F.D.M. Canedo ¹⁰⁸, M. Carabas ¹²², F. Carnesecchi ²⁵, R. Caron ^{124,126}, J. Castillo Castellanos ¹²⁶, F. Catalano ²⁹, C. Ceballos Sanchez ¹³⁹, I. Chakaberia ⁷³, P. Chakraborty ⁴⁵, S. Chandra ¹³⁰, S. Chapelain ³², M. Chartier ¹¹⁵, S. Chattopadhyay ¹³⁰, S. Chattopadhyay ⁹⁸, T.G. Chavez ⁴³, T. Cheng ⁶, C. Cheshkov ¹²⁴, B. Cheynis ¹²⁴, V. Chibante Barroso ³², D.D. Chinellato ¹⁰⁹, E.S. Chizzali ^{II,95}, S. Cho ⁵⁶, P. Chochula ³², P. Christakoglou ⁸³, C.H. Christensen ⁸², P. Christiansen ⁷⁴, T. Chujo ¹²¹, M. Ciacco ²⁹, C. Cicalo ⁵⁰, L. Cifarelli ²⁵, F. Cindolo ⁴⁹, M.R. Ciupek ⁹⁷, G. Clai ^{III,49}, J. Cleymans ^{I,111}, F. Colamaria ⁴⁸, J.S. Colburn ⁹⁹, D. Colella ⁴⁸, A. Collu ⁷³, M. Colocci ³², M. Concas ^{IV,54}, G. Conesa Balbastre ⁷², Z. Conesa del Valle ⁷¹, G. Contin ²³, J.G. Contreras ³⁵, M.L. Coquet ¹²⁶, T.M. Cormier ^{I,86}, P. Cortese ¹²⁸, M.R. Cosentino ¹¹⁰, F. Costa ³², S. Costanza ^{21,53}, P. Crochet ¹²³, R. Cruz-Torres ⁷³, E. Cuautle ⁶³, P. Cui ⁶, L. Cunqueiro ⁸⁶, A. Dainese ⁵², M.C. Danisch ⁹⁴, A. Danu ⁶¹, P. Das ⁷⁹, P. Das ⁴, S. Das ⁴, S. Dash ⁴⁵, R.M.H. David ⁴³, A. De Caro ²⁸, G. de Cataldo ⁴⁸, L. De Cilladi ²⁴, J. de Cuveland ³⁷, A. De Falco ²², D. De Gruttola ²⁸, N. De Marco ⁵⁴, C. De Martin ²³, S. De Pasquale ²⁸, S. Deb ⁴⁶, H.F. Degenhardt ¹⁰⁸, K.R. Deja ¹³¹, R. Del Grande ⁹⁵, L. Dello Stritto ²⁸, W. Deng ⁶, P. Dhankher ¹⁸, D. Di Bari ³¹, A. Di Mauro ³², R.A. Diaz ^{139,7}, T. Dietel ¹¹¹, Y. Ding ^{124,6}, R. Divià ³², D.U. Dixit ¹⁸, Ø. Djupsland ²⁰, U. Dmitrieva ¹³⁸, A. Dobrin ⁶¹, B. Dönigus ⁶², A.K. Dubey ¹³⁰, J.M. Dubinski ¹³¹, A. Dubla ^{97,83}, S. Dudi ⁸⁹, P. Dupieux ¹²³, M. Durkac ¹⁰⁴, N. Dzalaiova ¹², T.M. Eder ¹³³, R.J. Ehlers ⁸⁶, V.N. Eikeland ²⁰, F. Eisenhut ⁶², D. Elia ⁴⁸, B. Erazmus ¹⁰², F. Ercolelli ²⁵, F. Erhardt ⁸⁸, A. Erokhin ¹³⁸, M.R. Ersdal ²⁰, B. Espagnon ⁷¹, G. Eulisse ³², D. Evans ⁹⁹, S. Evdokimov ¹³⁸, L. Fabbietti ⁹⁵, M. Faggin ²⁷, J. Faivre ⁷², F. Fan ⁶, W. Fan ⁷³, A. Fantoni ⁴⁷, M. Fasel ⁸⁶, P. Fecchio ²⁹, A. Feliciello ⁵⁴, G. Feofilov ¹³⁸, A. Fernández Téllez ⁴³, A. Ferrero ¹²⁶, A. Ferretti ²⁴, V.J.G. Feuillard ⁹⁴, J. Figiel ¹⁰⁵, V. Filova ³⁵, D. Finogeev ¹³⁸, G. Fiorenza ⁹⁶, F. Flor ¹¹², A.N. Flores ¹⁰⁶, S. Foertsch ⁶⁶, I. Fokin ⁹⁴, S. Fokin ¹³⁸, E. Fragiocomo ⁵⁵, E. Frajna ¹³⁴, U. Fuchs ³², N. Funicello ²⁸, C. Furget ⁷², A. Furs ¹³⁸, J.J. Gaardhøje ⁸², M. Gagliardi ²⁴, A.M. Gago ¹⁰⁰, A. Gal ¹²⁵, C.D. Galvan ¹⁰⁷, P. Ganoti ⁷⁷, C. Garabatos ⁹⁷, J.R.A. Garcia ⁴³, E. Garcia-Solis ⁹, K. Garg ¹⁰², C. Gargiulo ³², A. Garibaldi ⁸⁰, K. Garner ¹³³, E.F. Gauger ¹⁰⁶, A. Gautam ¹¹⁴, M.B. Gay Ducati ⁶⁴, M. Germain ¹⁰², S.K. Ghosh ⁴, M. Giacalone ²⁵, P. Gianotti ⁴⁷, P. Giubellino ^{97,54}, P. Giubilato ²⁷, A.M.C. Glaenzer ¹²⁶, P. Glässel ⁹⁴, E. Glimos ¹¹⁸, D.J.Q. Goh ⁷⁵, V. Gonzalez ¹³², L.H. González-Trueba ⁶⁵, S. Gorbunov ³⁷, M. Gorgon ², L. Görlich ¹⁰⁵, S. Gotovac ³³, V. Grabski ⁶⁵, L.K. Graczykowski ¹³¹, E. Grecka ⁸⁵, L. Greiner ⁷³, A. Grelli ⁵⁷, C. Grigoras ³², V. Grigoriev ¹³⁸, S. Grigoryan ^{139,1}, F. Grossa ⁵⁴, J.F. Grosse-Oetringhaus ³², R. Grossi ⁹⁷, D. Grund ³⁵, G.G. Guardiano ¹⁰⁹, R. Guernane ⁷², M. Guilbaud ¹⁰², K. Gulbrandsen ⁸², T. Gunji ¹²⁰, W. Guo ⁶, A. Gupta ⁹⁰, R. Gupta ⁹⁰,

- S.P. Guzman ⁴³, L. Gyulai ¹³⁴, M.K. Habib⁹⁷, C. Hadjidakis ⁷¹, H. Hamagaki ⁷⁵, M. Hamid⁶, R. Hannigan ¹⁰⁶, M.R. Haque ¹³¹, A. Harlenderova ⁹⁷, J.W. Harris ¹³⁵, A. Harton ⁹, J.A. Hasenbichler ³², H. Hassan ⁸⁶, D. Hatzifotiadou ⁴⁹, P. Hauer ⁴¹, L.B. Havener ¹³⁵, S.T. Heckel ⁹⁵, E. Hellbär ⁹⁷, H. Helstrup ³⁴, T. Herman ³⁵, G. Herrera Corral ⁸, F. Herrmann ¹³³, K.F. Hetland ³⁴, B. Heybeck ⁶², H. Hillemanns ³², C. Hills ¹¹⁵, B. Hippolyte ¹²⁵, B. Hofman ⁵⁷, B. Hohlweger ⁸³, J. Honermann ¹³³, G.H. Hong ¹³⁶, D. Horak ³⁵, A. Horzyk ², R. Hosokawa ¹⁴, Y. Hou ⁶, P. Hristov ³², C. Hughes ¹¹⁸, P. Huhn ⁶², L.M. Huhta ¹¹³, C.V. Hulse ⁷¹, T.J. Humanic ⁸⁷, H. Hushnud ⁹⁸, A. Hutson ¹¹², D. Hutter ³⁷, J.P. Iddon ¹¹⁵, R. Ilkaev ¹³⁸, H. Ilyas ¹³, M. Inaba ¹²¹, G.M. Innocenti ³², M. Ippolitov ¹³⁸, A. Isakov ⁸⁵, T. Isidori ¹¹⁴, M.S. Islam ⁹⁸, M. Ivanov ⁹⁷, V. Ivanov ¹³⁸, V. Izucheev ¹³⁸, M. Jablonski ², B. Jacak ⁷³, N. Jacazio ³², P.M. Jacobs ⁷³, S. Jadlovska ¹⁰⁴, J. Jadlovsky ¹⁰⁴, C. Jahnke ¹⁰⁹, A. Jalotra ⁹⁰, M.A. Janik ¹³¹, T. Janson ⁶⁸, M. Jercic ⁸⁸, O. Jevons ⁹⁹, A.A.P. Jimenez ⁶³, F. Jonas ^{86,133}, P.G. Jones ⁹⁹, J.M. Jowett ^{32,97}, J. Jung ⁶², M. Jung ⁶², A. Junique ³², A. Jusko ⁹⁹, M.J. Kabus ¹³¹, J. Kaewjai ¹⁰³, P. Kalinak ⁵⁸, A.S. Kalteyer ⁹⁷, A. Kalweit ³², V. Kaplin ¹³⁸, A. Karasu Uysal ⁷⁰, D. Karatovic ⁸⁸, O. Karavichev ¹³⁸, T. Karavicheva ¹³⁸, P. Karczmarczyk ¹³¹, E. Karpechev ¹³⁸, V. Kashyap ⁷⁹, A. Kazantsev ¹³⁸, U. Kebschull ⁶⁸, R. Keidel ¹³⁷, D.L.D. Keijdener ⁵⁷, M. Keil ³², B. Ketzer ⁴¹, A.M. Khan ⁶, S. Khan ¹⁵, A. Khanzadeev ¹³⁸, Y. Kharlov ¹³⁸, A. Khatun ¹⁵, A. Khuntia ¹⁰⁵, B. Kileng ³⁴, B. Kim ¹⁶, C. Kim ¹⁶, D.J. Kim ¹¹³, E.J. Kim ⁶⁷, J. Kim ¹³⁶, J.S. Kim ³⁹, J. Kim ⁹⁴, J. Kim ⁶⁷, M. Kim ⁹⁴, S. Kim ¹⁷, T. Kim ¹³⁶, S. Kirsch ⁶², I. Kisel ³⁷, S. Kiselev ¹³⁸, A. Kisiel ¹³¹, J.P. Kitowski ², J.L. Klay ⁵, J. Klein ³², S. Klein ⁷³, C. Klein-Bösing ¹³³, M. Kleiner ⁶², T. Klemenz ⁹⁵, A. Kluge ³², A.G. Knospe ¹¹², C. Kobdaj ¹⁰³, T. Kollegger ⁹⁷, A. Kondratyev ¹³⁹, N. Kondratyeva ¹³⁸, E. Kondratyuk ¹³⁸, J. Konig ⁶², S.A. Konigstorfer ⁹⁵, P.J. Konopka ³², G. Kornakov ¹³¹, S.D. Koryciak ², A. Kotliarov ⁸⁵, O. Kovalenko ⁷⁸, V. Kovalenko ¹³⁸, M. Kowalski ¹⁰⁵, I. Králik ⁵⁸, A. Kravčáková ³⁶, L. Kreis ⁹⁷, M. Krivda ^{99,58}, F. Krizek ⁸⁵, K. Krizkova Gajdosova ³⁵, M. Kroesen ⁹⁴, M. Krüger ⁶², D.M. Krupova ³⁵, E. Kryshen ¹³⁸, M. Krzewicki ³⁷, V. Kučera ³², C. Kuhn ¹²⁵, P.G. Kuijer ⁸³, T. Kumaoka ¹²¹, D. Kumar ¹³⁰, L. Kumar ⁸⁹, N. Kumar ⁸⁹, S. Kundu ³², P. Kurashvili ⁷⁸, A. Kurepin ¹³⁸, A.B. Kurepin ¹³⁸, A. Kuryakin ¹³⁸, S. Kushpil ⁸⁵, J. Kvapil ⁹⁹, M.J. Kweon ⁵⁶, J.Y. Kwon ⁵⁶, Y. Kwon ¹³⁶, S.L. La Pointe ³⁷, P. La Rocca ²⁶, Y.S. Lai ⁷³, A. Lakrathok ¹⁰³, M. Lamanna ³², R. Langoy ¹¹⁷, P. Larionov ⁴⁷, E. Laudi ³², L. Lautner ^{32,95}, R. Lavicka ^{101,35}, T. Lazareva ¹³⁸, R. Lea ^{129,53}, J. Lehrbach ³⁷, R.C. Lemmon ⁸⁴, I. León Monzón ¹⁰⁷, M.M. Lesch ⁹⁵, E.D. Lesser ¹⁸, M. Lettrich ^{32,95}, P. Lévai ¹³⁴, X. Li ¹⁰, X.L. Li ⁶, J. Lien ¹¹⁷, R. Lietava ⁹⁹, B. Lim ¹⁶, S.H. Lim ¹⁶, V. Lindenstruth ³⁷, A. Lindner ⁴⁴, C. Lippmann ⁹⁷, A. Liu ¹⁸, D.H. Liu ⁶, J. Liu ¹¹⁵, I.M. Lofnes ²⁰, V. Loginov ¹³⁸, C. Loizides ⁸⁶, P. Loncar ³³, J.A. Lopez ⁹⁴, X. Lopez ¹²³, E. López Torres ⁷, P. Lu ¹¹⁶, J.R. Luhder ¹³³, M. Lunardon ²⁷, G. Luparello ⁵⁵, Y.G. Ma ³⁸, A. Maevskaya ¹³⁸, M. Mager ³², T. Mahmoud ⁴¹, A. Maire ¹²⁵, M. Malaev ¹³⁸, N.M. Malik ⁹⁰, Q.W. Malik ¹⁹, S.K. Malik ⁹⁰, L. Malinina ^{VII,139}, D. Mal'Kevich ¹³⁸, D. Mallick ⁷⁹, N. Mallick ⁴⁶, G. Mandaglio ^{30,51}, V. Manko ¹³⁸, F. Manso ¹²³, V. Manzari ⁴⁸, Y. Mao ⁶, G.V. Margagliotti ²³, A. Margotti ⁴⁹, A. Marín ⁹⁷, C. Markert ¹⁰⁶, M. Marquard ⁶², N.A. Martin ⁹⁴, P. Martinengo ³², J.L. Martinez ¹¹², M.I. Martínez ⁴³, G. Martínez García ¹⁰², S. Masciocchi ⁹⁷, M. Masera ²⁴, A. Masoni ⁵⁰, L. Massacrier ⁷¹, A. Mastroserio ^{127,48}, A.M. Mathis ⁹⁵, O. Matonoha ⁷⁴, P.F.T. Matuoka ¹⁰⁸, A. Matyja ¹⁰⁵, C. Mayer ¹⁰⁵, A.L. Mazuecos ³², F. Mazzaschi ²⁴, M. Mazzilli ³², J.E. Mdhhluli ¹¹⁹, A.F. Mechler ⁶², Y. Melikyan ¹³⁸, A. Menchaca-Rocha ⁶⁵, E. Meninno ^{101,28}, A.S. Menon ¹¹², M. Meres ¹², S. Mhlanga ^{111,66}, Y. Miake ¹²¹, L. Micheletti ⁵⁴, L.C. Migliorin ¹²⁴, D.L. Mihaylov ⁹⁵, K. Mikhaylov ^{139,138}, A.N. Mishra ¹³⁴, D. Miśkowiec ⁹⁷, A. Modak ⁴, A.P. Mohanty ⁵⁷, B. Mohanty ⁷⁹, M. Mohisin Khan ^{V,15}, M.A. Molander ⁴², Z. Moravcova ⁸², C. Mordasini ⁹⁵, D.A. Moreira De Godoy ¹³³, I. Morozov ¹³⁸, A. Morsch ³², T. Mrnjavac ³², V. Muccifora ⁴⁷, E. Mudnic ³³, S. Muhuri ¹³⁰, J.D. Mulligan ⁷³, A. Mulliri ²², M.G. Munhoz ¹⁰⁸, R.H. Munzer ⁶², H. Murakami ¹²⁰, S. Murray ¹¹¹, L. Musa ³², J. Musinsky ⁵⁸, J.W. Myrcha ¹³¹, B. Naik ¹¹⁹, R. Nair ⁷⁸, B.K. Nandi ⁴⁵, R. Nania ⁴⁹, E. Nappi ⁴⁸, A.F. Nassirpour ⁷⁴, A. Nath ⁹⁴, C. Nattrass ¹¹⁸, A. Neagu ¹⁹, A. Negru ¹²², L. Nellen ⁶³, S.V. Nesbo ³⁴, G. Neskovic ³⁷, D. Nesterov ¹³⁸, B.S. Nielsen ⁸², E.G. Nielsen ⁸², S. Nikolaev ¹³⁸, S. Nikulin ¹³⁸, V. Nikulin ¹³⁸, F. Noferini ⁴⁹, S. Noh ¹¹, P. Nomokonov ¹³⁹, J. Norman ¹¹⁵, N. Novitzky ¹²¹, P. Nowakowski ¹³¹, A. Nyanin ¹³⁸, J. Nystrand ²⁰, M. Ogino ⁷⁵, A. Ohlson ⁷⁴, V.A. Okorokov ¹³⁸, J. Oleniacz ¹³¹, A.C. Oliveira Da Silva ¹¹⁸, M.H. Oliver ¹³⁵, A. Onnerstad ¹¹³, C. Oppedisano ⁵⁴, A. Ortiz Velasquez ⁶³, A. Oskarsson ⁷⁴, J. Otwinowski ¹⁰⁵, M. Oya ⁹², K. Oyama ⁷⁵, Y. Pachmayer ⁹⁴, S. Padhan ⁴⁵, D. Pagano ^{129,53}, G. Paić ⁶³, A. Palasciano ⁴⁸, S. Panebianco ¹²⁶, J. Park ⁵⁶, J.E. Parkkila ^{32,113}, S.P. Pathak ¹¹², R.N. Patra ³², B. Paul ²², H. Pei ⁶, T. Peitzmann ⁵⁷, X. Peng ⁶, L.G. Pereira ⁶⁴, H. Pereira Da Costa ¹²⁶, D. Peresunko ¹³⁸, G.M. Perez ⁷, S. Perrin ¹²⁶, Y. Pestov ¹³⁸,

- V. Petráček ³⁵, V. Petrov ¹³⁸, M. Petrovici ⁴⁴, R.P. Pezzi ⁶⁴, S. Piano ⁵⁵, M. Pikna ¹², P. Pillot ¹⁰², O. Pinazza ^{49,32}, L. Pinsky ¹¹², C. Pinto ^{95,26}, S. Pisano ⁴⁷, M. Płoskoń ⁷³, M. Planinic ⁸⁸, F. Pliquet ⁶², M.G. Poghosyan ⁸⁶, B. Polichtchouk ¹³⁸, S. Politano ²⁹, N. Poljak ⁸⁸, A. Pop ⁴⁴, S. Porteboeuf-Houssais ¹²³, J. Porter ⁷³, V. Pozdniakov ¹³⁹, S.K. Prasad ⁴, R. Preghenella ⁴⁹, F. Prino ⁵⁴, C.A. Pruneau ¹³², I. Pshenichnov ¹³⁸, M. Puccio ³², S. Qiu ⁸³, L. Quaglia ²⁴, R.E. Quishpe ¹¹², S. Ragoni ⁹⁹, A. Rakotozafindrabe ¹²⁶, L. Ramello ¹²⁸, F. Rami ¹²⁵, S.A.R. Ramirez ⁴³, T.A. Rancien ⁷², R. Raniwala ⁹¹, S. Raniwala ⁹¹, S.S. Räsänen ⁴², R. Rath ⁴⁶, I. Ravasenga ⁸³, K.F. Read ^{86,118}, A.R. Redelbach ³⁷, K. Redlich ^{VI,78}, A. Rehman ²⁰, P. Reichelt ⁶², F. Reidt ³², H.A. Reme-Ness ³⁴, Z. Rescakova ³⁶, K. Reygers ⁹⁴, A. Riabov ¹³⁸, V. Riabov ¹³⁸, R. Ricci ²⁸, T. Richert ⁷⁴, M. Richter ¹⁹, W. Riegler ³², F. Riggi ²⁶, C. Ristea ⁶¹, M. Rodríguez Cahuantzi ⁴³, K. Røed ¹⁹, R. Rogalev ¹³⁸, E. Rogochaya ¹³⁹, T.S. Rogoschinski ⁶², D. Rohr ³², D. Röhrich ²⁰, P.F. Rojas ⁴³, S. Rojas Torres ³⁵, P.S. Rokita ¹³¹, F. Ronchetti ⁴⁷, A. Rosano ^{30,51}, E.D. Rosas ⁶³, A. Rossi ⁵², A. Roy ⁴⁶, P. Roy ⁹⁸, S. Roy ⁴⁵, N. Rubini ²⁵, O.V. Rueda ⁷⁴, D. Ruggiano ¹³¹, R. Rui ²³, B. Rumyantsev ¹³⁹, P.G. Russek ², R. Russo ⁸³, A. Rustamov ⁸⁰, E. Ryabinkin ¹³⁸, Y. Ryabov ¹³⁸, A. Rybicki ¹⁰⁵, H. Rytkonen ¹¹³, W. Rzesz ¹³¹, O.A.M. Saarimaki ⁴², R. Sadek ¹⁰², S. Sadovsky ¹³⁸, J. Saetre ²⁰, K. Šafařík ³⁵, S.K. Saha ¹³⁰, S. Saha ⁷⁹, B. Sahoo ⁴⁵, P. Sahoo ⁴⁵, R. Sahoo ⁴⁶, S. Sahoo ⁵⁹, D. Sahu ⁴⁶, P.K. Sahu ⁵⁹, J. Saini ¹³⁰, S. Sakai ¹²¹, M.P. Salván ⁹⁷, S. Sambyal ⁹⁰, T.B. Saramela ¹⁰⁸, D. Sarkar ¹³², N. Sarkar ¹³⁰, P. Sarma ⁴⁰, V.M. Sarti ⁹⁵, M.H.P. Sas ¹³⁵, J. Schambach ⁸⁶, H.S. Scheid ⁶², C. Schiaua ⁴⁴, R. Schicker ⁹⁴, A. Schmah ⁹⁴, C. Schmidt ⁹⁷, H.R. Schmidt ⁹³, M.O. Schmidt ³², M. Schmidt ⁹³, N.V. Schmidt ^{86,62}, A.R. Schmier ¹¹⁸, R. Schotter ¹²⁵, J. Schukraft ³², K. Schwarz ⁹⁷, K. Schweda ⁹⁷, G. Scioli ²⁵, E. Scomparin ⁵⁴, J.E. Seger ¹⁴, Y. Sekiguchi ¹²⁰, D. Sekihata ¹²⁰, I. Selyuzhenkov ^{97,138}, S. Senyukov ¹²⁵, J.J. Seo ⁵⁶, D. Serebryakov ¹³⁸, L. Šerkšnytė ⁹⁵, A. Sevcenco ⁶¹, T.J. Shaba ⁶⁶, A. Shabanov ¹³⁸, A. Shabetai ¹⁰², R. Shahoyan ³², W. Shaikh ⁹⁸, A. Shangaraev ¹³⁸, A. Sharma ⁸⁹, D. Sharma ⁴⁵, H. Sharma ¹⁰⁵, M. Sharma ⁹⁰, N. Sharma ⁸⁹, S. Sharma ⁹⁰, U. Sharma ⁹⁰, A. Shatat ⁷¹, O. Sheibani ¹¹², K. Shigaki ⁹², M. Shimomura ⁷⁶, S. Shirinkin ¹³⁸, Q. Shou ³⁸, Y. Sibiriak ¹³⁸, S. Siddhanta ⁵⁰, T. Siemiarczuk ⁷⁸, T.F. Silva ¹⁰⁸, D. Silvermyr ⁷⁴, T. Simantathammakul ¹⁰³, G. Simonetti ³², B. Singh ⁹⁵, R. Singh ⁷⁹, R. Singh ⁹⁰, R. Singh ⁴⁶, V.K. Singh ¹³⁰, V. Singhal ¹³⁰, T. Sinha ⁹⁸, B. Sitar ¹², M. Sitta ¹²⁸, T.B. Skaali ¹⁹, G. Skorodumovs ⁹⁴, M. Slupecki ⁴², N. Smirnov ¹³⁵, R.J.M. Snellings ⁵⁷, C. Soncco ¹⁰⁰, J. Song ¹¹², A. Songmoolnak ¹⁰³, F. Soramel ²⁷, S. Sorensen ¹¹⁸, I. Sputowska ¹⁰⁵, J. Stachel ⁹⁴, I. Stan ⁶¹, P.J. Steffanic ¹¹⁸, S.F. Stiefelmaier ⁹⁴, D. Stocco ¹⁰², I. Storehaug ¹⁹, M.M. Storetvedt ³⁴, P. Stratmann ¹³³, S. Strazzi ²⁵, C.P. Stylianidis ⁸³, A.A.P. Suáide ¹⁰⁸, C. Suire ⁷¹, M. Sukhanov ¹³⁸, M. Suljic ³², R. Sultanov ¹³⁸, V. Sumberia ⁹⁰, S. Sumowidagdo ⁸¹, S. Swain ⁵⁹, A. Szabo ¹², I. Szarka ¹², U. Tabassam ¹³, S.F. Taghavi ⁹⁵, G. Taillepied ^{97,123}, J. Takahashi ¹⁰⁹, G.J. Tambave ²⁰, S. Tang ^{123,6}, Z. Tang ¹¹⁶, J.D. Tapia Takaki ¹¹⁴, N. Tapus ¹²², L.A. Tarasovicova ¹³³, M.G. Tarzila ⁴⁴, A. Tauro ³², G. Tejeda Muñoz ⁴³, A. Telesca ³², L. Terlizzi ²⁴, C. Terrevoli ¹¹², G. Tersimonov ³, S. Thakur ¹³⁰, D. Thomas ¹⁰⁶, R. Tieulent ¹²⁴, A. Tikhonov ¹³⁸, A.R. Timmins ¹¹², M. Tkacik ¹⁰⁴, T. Tkacik ¹⁰⁴, A. Toia ⁶², N. Topilskaya ¹³⁸, M. Toppi ⁴⁷, F. Torales-Acosta ¹⁸, T. Tork ⁷¹, A.G. Torres Ramos ³¹, A. Trifiró ^{30,51}, A.S. Triolo ^{30,51}, S. Tripathy ⁴⁹, T. Tripathy ⁴⁵, S. Trogolo ³², V. Trubnikov ³, W.H. Trzaska ¹¹³, T.P. Trzciński ¹³¹, A. Tumkin ¹³⁸, R. Turrisi ⁵², T.S. Tveter ¹⁹, K. Ullaland ²⁰, A. Uras ¹²⁴, M. Urioni ^{53,129}, G.L. Usai ²², M. Vala ³⁶, N. Valle ²¹, S. Vallero ⁵⁴, L.V.R. van Doremalen ⁵⁷, M. van Leeuwen ⁸³, R.J.G. van Weelden ⁸³, P. Vande Vyvre ³², D. Varga ¹³⁴, Z. Varga ¹³⁴, M. Varga-Kofarago ¹³⁴, M. Vasileiou ⁷⁷, A. Vasiliev ¹³⁸, O. Vázquez Doce ⁹⁵, V. Vechernin ¹³⁸, E. Vercellin ²⁴, S. Vergara Limón ⁴³, L. Vermunt ⁵⁷, R. Vértesi ¹³⁴, M. Verweij ⁵⁷, L. Vickovic ³³, Z. Vilakazi ¹¹⁹, O. Villalobos Baillie ⁹⁹, G. Vino ⁴⁸, A. Vinogradov ¹³⁸, T. Virgili ²⁸, V. Vislavicius ⁸², A. Vodopjanov ¹³⁹, B. Volkel ³², M.A. Völkli ⁹⁴, K. Voloshin ¹³⁸, S.A. Voloshin ¹³², G. Volpe ³¹, B. von Haller ³², I. Vorobyev ⁹⁵, N. Vozniuk ¹³⁸, J. Vrláková ³⁶, B. Wagner ²⁰, C. Wang ³⁸, D. Wang ³⁸, M. Weber ¹⁰¹, A. Wegrzynek ³², F.T. Weiglhofer ³⁷, S.C. Wenzel ³², J.P. Wessels ¹³³, S.L. Weyhmiller ¹³⁵, J. Wiechula ⁶², J. Wikne ¹⁹, G. Wilk ⁷⁸, J. Wilkinson ⁹⁷, G.A. Willems ¹³³, B. Windelband ⁹⁴, M. Winn ¹²⁶, W.E. Witt ¹¹⁸, J.R. Wright ¹⁰⁶, W. Wu ³⁸, Y. Wu ¹¹⁶, R. Xu ⁶, A.K. Yadav ¹³⁰, S. Yalein ⁷⁰, Y. Yamaguchi ⁹², K. Yamakawa ⁹², S. Yang ²⁰, S. Yano ⁹², Z. Yin ⁶, I.-K. Yoo ¹⁶, J.H. Yoon ⁵⁶, S. Yuan ²⁰, A. Yuncu ⁹⁴, V. Zaccolo ²³, C. Zampolli ³², H.J.C. Zanolli ⁵⁷, F. Zanone ⁹⁴, N. Zardoshti ^{32,99}, A. Zarochentsev ¹³⁸, P. Závada ⁶⁰, N. Zaviyalov ¹³⁸, M. Zhalov ¹³⁸, B. Zhang ⁶, S. Zhang ³⁸, X. Zhang ⁶, Y. Zhang ¹¹⁶, M. Zhao ¹⁰, V. Zherebchevskii ¹³⁸, Y. Zhi ¹⁰, N. Zhigareva ¹³⁸, D. Zhou ⁶, Y. Zhou ⁸², J. Zhu ^{97,6}, Y. Zhu ⁶, G. Zinovjev ^{1,3}, N. Zurlo ^{129,53}

Affiliation Notes

¹ Deceased

^{II} Also at: Max-Planck-Institut für Physik, Munich, Germany

^{III} Also at: Italian National Agency for New Technologies, Energy and Sustainable Economic Development (ENEA), Bologna, Italy

^{IV} Also at: Dipartimento DET del Politecnico di Torino, Turin, Italy

^V Also at: Department of Applied Physics, Aligarh Muslim University, Aligarh, India

^{VI} Also at: Institute of Theoretical Physics, University of Wroclaw, Poland

^{VII} Also at: An institution covered by a cooperation agreement with CERN

Collaboration Institutes

¹ A.I. Alikhanyan National Science Laboratory (Yerevan Physics Institute) Foundation, Yerevan, Armenia

² AGH University of Science and Technology, Cracow, Poland

³ Bogolyubov Institute for Theoretical Physics, National Academy of Sciences of Ukraine, Kiev, Ukraine

⁴ Bose Institute, Department of Physics and Centre for Astroparticle Physics and Space Science (CAPSS), Kolkata, India

⁵ California Polytechnic State University, San Luis Obispo, California, United States

⁶ Central China Normal University, Wuhan, China

⁷ Centro de Aplicaciones Tecnológicas y Desarrollo Nuclear (CEADEN), Havana, Cuba

⁸ Centro de Investigación y de Estudios Avanzados (CINVESTAV), Mexico City and Mérida, Mexico

⁹ Chicago State University, Chicago, Illinois, United States

¹⁰ China Institute of Atomic Energy, Beijing, China

¹¹ Chungbuk National University, Cheongju, Republic of Korea

¹² Comenius University Bratislava, Faculty of Mathematics, Physics and Informatics, Bratislava, Slovak Republic

¹³ COMSATS University Islamabad, Islamabad, Pakistan

¹⁴ Creighton University, Omaha, Nebraska, United States

¹⁵ Department of Physics, Aligarh Muslim University, Aligarh, India

¹⁶ Department of Physics, Pusan National University, Pusan, Republic of Korea

¹⁷ Department of Physics, Sejong University, Seoul, Republic of Korea

¹⁸ Department of Physics, University of California, Berkeley, California, United States

¹⁹ Department of Physics, University of Oslo, Oslo, Norway

²⁰ Department of Physics and Technology, University of Bergen, Bergen, Norway

²¹ Dipartimento di Fisica, Università di Pavia, Pavia, Italy

²² Dipartimento di Fisica dell'Università and Sezione INFN, Cagliari, Italy

²³ Dipartimento di Fisica dell'Università and Sezione INFN, Trieste, Italy

²⁴ Dipartimento di Fisica dell'Università and Sezione INFN, Turin, Italy

²⁵ Dipartimento di Fisica e Astronomia dell'Università and Sezione INFN, Bologna, Italy

²⁶ Dipartimento di Fisica e Astronomia dell'Università and Sezione INFN, Catania, Italy

²⁷ Dipartimento di Fisica e Astronomia dell'Università and Sezione INFN, Padova, Italy

²⁸ Dipartimento di Fisica 'E.R. Caianiello' dell'Università and Gruppo Collegato INFN, Salerno, Italy

²⁹ Dipartimento DISAT del Politecnico and Sezione INFN, Turin, Italy

³⁰ Dipartimento di Scienze MIFT, Università di Messina, Messina, Italy

³¹ Dipartimento Interateneo di Fisica 'M. Merlin' and Sezione INFN, Bari, Italy

³² European Organization for Nuclear Research (CERN), Geneva, Switzerland

³³ Faculty of Electrical Engineering, Mechanical Engineering and Naval Architecture, University of Split, Split, Croatia

³⁴ Faculty of Engineering and Science, Western Norway University of Applied Sciences, Bergen, Norway

³⁵ Faculty of Nuclear Sciences and Physical Engineering, Czech Technical University in Prague, Prague, Czech Republic

³⁶ Faculty of Science, P.J. Šafárik University, Košice, Slovak Republic

³⁷ Frankfurt Institute for Advanced Studies, Johann Wolfgang Goethe-Universität Frankfurt, Frankfurt, Germany

³⁸ Fudan University, Shanghai, China

³⁹ Gangneung-Wonju National University, Gangneung, Republic of Korea

⁴⁰ Gauhati University, Department of Physics, Guwahati, India

⁴¹ Helmholtz-Institut für Strahlen- und Kernphysik, Rheinische Friedrich-Wilhelms-Universität Bonn, Bonn,

Germany

- ⁴² Helsinki Institute of Physics (HIP), Helsinki, Finland
⁴³ High Energy Physics Group, Universidad Autónoma de Puebla, Puebla, Mexico
⁴⁴ Horia Hulubei National Institute of Physics and Nuclear Engineering, Bucharest, Romania
⁴⁵ Indian Institute of Technology Bombay (IIT), Mumbai, India
⁴⁶ Indian Institute of Technology Indore, Indore, India
⁴⁷ INFN, Laboratori Nazionali di Frascati, Frascati, Italy
⁴⁸ INFN, Sezione di Bari, Bari, Italy
⁴⁹ INFN, Sezione di Bologna, Bologna, Italy
⁵⁰ INFN, Sezione di Cagliari, Cagliari, Italy
⁵¹ INFN, Sezione di Catania, Catania, Italy
⁵² INFN, Sezione di Padova, Padova, Italy
⁵³ INFN, Sezione di Pavia, Pavia, Italy
⁵⁴ INFN, Sezione di Torino, Turin, Italy
⁵⁵ INFN, Sezione di Trieste, Trieste, Italy
⁵⁶ Inha University, Incheon, Republic of Korea
⁵⁷ Institute for Gravitational and Subatomic Physics (GRASP), Utrecht University/Nikhef, Utrecht, Netherlands
⁵⁸ Institute of Experimental Physics, Slovak Academy of Sciences, Košice, Slovak Republic
⁵⁹ Institute of Physics, Homi Bhabha National Institute, Bhubaneswar, India
⁶⁰ Institute of Physics of the Czech Academy of Sciences, Prague, Czech Republic
⁶¹ Institute of Space Science (ISS), Bucharest, Romania
⁶² Institut für Kernphysik, Johann Wolfgang Goethe-Universität Frankfurt, Frankfurt, Germany
⁶³ Instituto de Ciencias Nucleares, Universidad Nacional Autónoma de México, Mexico City, Mexico
⁶⁴ Instituto de Física, Universidade Federal do Rio Grande do Sul (UFRGS), Porto Alegre, Brazil
⁶⁵ Instituto de Física, Universidad Nacional Autónoma de México, Mexico City, Mexico
⁶⁶ iThemba LABS, National Research Foundation, Somerset West, South Africa
⁶⁷ Jeonbuk National University, Jeonju, Republic of Korea
⁶⁸ Johann-Wolfgang-Goethe Universität Frankfurt Institut für Informatik, Fachbereich Informatik und Mathematik, Frankfurt, Germany
⁶⁹ Korea Institute of Science and Technology Information, Daejeon, Republic of Korea
⁷⁰ KTO Karatay University, Konya, Turkey
⁷¹ Laboratoire de Physique des 2 Infinis, Irène Joliot-Curie, Orsay, France
⁷² Laboratoire de Physique Subatomique et de Cosmologie, Université Grenoble-Alpes, CNRS-IN2P3, Grenoble, France
⁷³ Lawrence Berkeley National Laboratory, Berkeley, California, United States
⁷⁴ Lund University Department of Physics, Division of Particle Physics, Lund, Sweden
⁷⁵ Nagasaki Institute of Applied Science, Nagasaki, Japan
⁷⁶ Nara Women's University (NWU), Nara, Japan
⁷⁷ National and Kapodistrian University of Athens, School of Science, Department of Physics , Athens, Greece
⁷⁸ National Centre for Nuclear Research, Warsaw, Poland
⁷⁹ National Institute of Science Education and Research, Homi Bhabha National Institute, Jatni, India
⁸⁰ National Nuclear Research Center, Baku, Azerbaijan
⁸¹ National Research and Innovation Agency - BRIN, Jakarta, Indonesia
⁸² Niels Bohr Institute, University of Copenhagen, Copenhagen, Denmark
⁸³ Nikhef, National institute for subatomic physics, Amsterdam, Netherlands
⁸⁴ Nuclear Physics Group, STFC Daresbury Laboratory, Daresbury, United Kingdom
⁸⁵ Nuclear Physics Institute of the Czech Academy of Sciences, Husinec-Řež, Czech Republic
⁸⁶ Oak Ridge National Laboratory, Oak Ridge, Tennessee, United States
⁸⁷ Ohio State University, Columbus, Ohio, United States
⁸⁸ Physics department, Faculty of science, University of Zagreb, Zagreb, Croatia
⁸⁹ Physics Department, Panjab University, Chandigarh, India
⁹⁰ Physics Department, University of Jammu, Jammu, India
⁹¹ Physics Department, University of Rajasthan, Jaipur, India
⁹² Physics Program and International Institute for Sustainability with Knotted Chiral Meta Matter (SKCM2), Hiroshima University, Hiroshima, Japan
⁹³ Physikalisches Institut, Eberhard-Karls-Universität Tübingen, Tübingen, Germany

- ⁹⁴ Physikalisches Institut, Ruprecht-Karls-Universität Heidelberg, Heidelberg, Germany
⁹⁵ Physik Department, Technische Universität München, Munich, Germany
⁹⁶ Politecnico di Bari and Sezione INFN, Bari, Italy
⁹⁷ Research Division and ExtreMe Matter Institute EMMI, GSI Helmholtzzentrum für Schwerionenforschung GmbH, Darmstadt, Germany
⁹⁸ Saha Institute of Nuclear Physics, Homi Bhabha National Institute, Kolkata, India
⁹⁹ School of Physics and Astronomy, University of Birmingham, Birmingham, United Kingdom
¹⁰⁰ Sección Física, Departamento de Ciencias, Pontificia Universidad Católica del Perú, Lima, Peru
¹⁰¹ Stefan Meyer Institut für Subatomare Physik (SMI), Vienna, Austria
¹⁰² SUBATECH, IMT Atlantique, Nantes Université, CNRS-IN2P3, Nantes, France
¹⁰³ Suranaree University of Technology, Nakhon Ratchasima, Thailand
¹⁰⁴ Technical University of Košice, Košice, Slovak Republic
¹⁰⁵ The Henryk Niewodniczanski Institute of Nuclear Physics, Polish Academy of Sciences, Cracow, Poland
¹⁰⁶ The University of Texas at Austin, Austin, Texas, United States
¹⁰⁷ Universidad Autónoma de Sinaloa, Culiacán, Mexico
¹⁰⁸ Universidade de São Paulo (USP), São Paulo, Brazil
¹⁰⁹ Universidade Estadual de Campinas (UNICAMP), Campinas, Brazil
¹¹⁰ Universidade Federal do ABC, Santo André, Brazil
¹¹¹ University of Cape Town, Cape Town, South Africa
¹¹² University of Houston, Houston, Texas, United States
¹¹³ University of Jyväskylä, Jyväskylä, Finland
¹¹⁴ University of Kansas, Lawrence, Kansas, United States
¹¹⁵ University of Liverpool, Liverpool, United Kingdom
¹¹⁶ University of Science and Technology of China, Hefei, China
¹¹⁷ University of South-Eastern Norway, Kongsberg, Norway
¹¹⁸ University of Tennessee, Knoxville, Tennessee, United States
¹¹⁹ University of the Witwatersrand, Johannesburg, South Africa
¹²⁰ University of Tokyo, Tokyo, Japan
¹²¹ University of Tsukuba, Tsukuba, Japan
¹²² University Politehnica of Bucharest, Bucharest, Romania
¹²³ Université Clermont Auvergne, CNRS/IN2P3, LPC, Clermont-Ferrand, France
¹²⁴ Université de Lyon, CNRS/IN2P3, Institut de Physique des 2 Infinis de Lyon, Lyon, France
¹²⁵ Université de Strasbourg, CNRS, IPHC UMR 7178, F-67000 Strasbourg, France, Strasbourg, France
¹²⁶ Université Paris-Saclay Centre d'Etudes de Saclay (CEA), IRFU, Département de Physique Nucléaire (DPhN), Saclay, France
¹²⁷ Università degli Studi di Foggia, Foggia, Italy
¹²⁸ Università del Piemonte Orientale, Vercelli, Italy
¹²⁹ Università di Brescia, Brescia, Italy
¹³⁰ Variable Energy Cyclotron Centre, Homi Bhabha National Institute, Kolkata, India
¹³¹ Warsaw University of Technology, Warsaw, Poland
¹³² Wayne State University, Detroit, Michigan, United States
¹³³ Westfälische Wilhelms-Universität Münster, Institut für Kernphysik, Münster, Germany
¹³⁴ Wigner Research Centre for Physics, Budapest, Hungary
¹³⁵ Yale University, New Haven, Connecticut, United States
¹³⁶ Yonsei University, Seoul, Republic of Korea
¹³⁷ Zentrum für Technologie und Transfer (ZTT), Worms, Germany
¹³⁸ Affiliated with an institute covered by a cooperation agreement with CERN
¹³⁹ Affiliated with an international laboratory covered by a cooperation agreement with CERN.